Mechanical Systems and Signal Processing 146 (2021) 107011

Contents lists available at ScienceDirect

Mechanical Systems and Signal Processing

journal homepage: www.elsevier.com/locate/ymssp

An intelligent serial connected hybrid control method for gantry cranes

Hakan Yavuz [a], Serkan Beller [b,*]

[a] Faculty of Engineering, Mechanical Engineering Department, Çukurova University, Adana, Turkey
[b] İmamoğlu Technical Science College, Gas, and Fitting Technologies Department, Çukurova University, Adana, Turkey

ARTICLE INFO

Article history:
Received 26 November 2019
Received in revised form 8 April 2020
Accepted 27 May 2020
Available online 11 June 2020

Keywords:
Input Shaping
NN
GRNN
RBFN
Simple Pendulum

ABSTRACT

The cranes are usually controlled by a variety of actions including handling, lifting, carrying, then lowering and gripping the load. An intelligent control system could provide the operator with important advantages when performing all these operations. As the load cycle times are reduced, the operations are then performed more efficiently, and hence saving time, costs and increasing the overall productivity. As the control system optimizes the motion of the crane, the crane and its components are subjected to load and related stresses for shorter length of time leading to longer lifespans. Most importantly, the likelihood of human error is reduced and security is increased. Especially the transportation of fragile, sensitive materials or load transfer in dangerous conditions makes the operator control very difficult. The present study demonstrates how to perform a artificial intelligence assisted transport operation under variable conditions with hybrid control methods on a simple pendulum. Zero Vibration (ZV) input shaping (IS) method was implemented to a simple pendulum experiment setup with different heights and variable weights. Neural Network (NN), General Regression NN (GRNN), and Radial Basis Function Network (RBFN) were used with serial as a closed-loop intelligent control methods. The presented results indicate that the proposed approach constributes to the overall performance for elimination of residual vibrations.

© 2020 Elsevier Ltd. All rights reserved.

1. Introduction

Nowadays, there are many intelligent features that allow you to have more control over the loads on the crane and the crane than ever before. These intelligent features help to streamline lifting and transport operations, make use of crane easier and provide shorter cycle times. This makes cranes safer and easier to use. For example, swing control reduces the load swing, prevents stumbling and stops the crane if it is fitted. The assisted load rotation prevention reduces tilting. Defining and controlling the protected areas helps to keep the work area of the crane more secure and provides precise positioning thereby improving final load positioning. In addition to these, some other control technologies are shock load blocking, loose rope blocking, hook synchronization, distance adjustment control, micro speed, extended speed range, target positioning, final positioning and working area limits. These features provide optimization of maintenance activities in methods, such

* Corresponding author.
E-mail addresses: hyavuz@cu.edu.tr (H. Yavuz), sbeller@cu.edu.tr (S. Beller).

https://doi.org/10.1016/j.ymssp.2020.107011
0888-3270/© 2020 Elsevier Ltd. All rights reserved.

as remote monitoring, provide visibility on maintenance, application compatibility issues and provides usage data. With the analysis of the usage data, an accurate planning about productivity and maintenance decisions are made [1].

The crane control systems are vitally important for carrying the payloads at the highest efficiency levels [2]. The operator's performance is also highly important, however it is hard to estimate in advance as it is defined by the operators mood, health and so on. At the same time, the operator must be capable of solving the problems in crane control. It is a difficult task to both keep efficiency high, ensure job safety and deal with technical problems all at once [3]. Therefore, using intelligent auxiliary control systems to asist the operator is important for the improvement of system performance [4] and elimination of the error rates. In addition, these intelligent features increase the safety and efficiency of the crane operator and enable the operator to make soft and controlled movements on the crane more easily. The automatic features used in these methods enable the crane operators to pay more attention to the surrounding working environment and to ensure safer and more productive operations while increasing efficiency and precision [1].

The basic expectation from the control systems is that the audited system must perform the specified task and can do it under all conditions. In doing so, the control systems either keep the values of the controlled quantities constant or vary them in a predetermined manner. The control systems are divided into two main classes in terms of audit effect. These are open-loop (OL) control systems (CSs) and closed-loop (CL) CSs. The basic difference between these two systems is the feedback effect. In OL-CSs, the control activity is detached from the system output and the output is not measured and there is no feedback. Therefore, the input is not determined by considering the system output information. In practice, OL-CSs are used in systems where the input and output connections are pre-defined and are not exposed to internal or external disturbances. Therefore, the CSs operate either on a scheduled or on a sequenced basis. The control signal in CL-CSs determined by using the system output information. The output of the system is evaluated and then checked with the reference input value. Thus, the input takes into account of the output of the system. Since the system output is fed back to the controller, such systems are also called feedback systems [5].

In this paper, initially, section two presents comparison tables about input shaping and hybrid control methods for the simple single pendulum cart crane systems. In section three, provides details on the materials of the experiment set, control chart and intelligent methods. In section four, experiment studies and graphical results are presented. The final section delivers the conclusions.

2. Previous studies

In literature, there are many studies presenting findings on position control of cranes. The Hybrid control methods are also reported among these studies. The variety of smart control methods has also led to the emergence of many hybrid control methods. Some of the input shaping based hybrid control methods for the cranes are mentioned in detail in Tables 1 and 2.

In the tables, the advantages and disadvantages details of each method relative to each other is presented. In this study, a single simple pendulum experiment set was modeled as a gantry crane. The ZV input shaping was used as the reference or base method and NN + GRNN was used as the auxiliary method. The benefit provided by the ZV input shaping method that the pendulum can perform the positioning work by itself with minimum oscillation with despite variable loads and heights. This allows automating the operation of the system. The oscillation period and damping ratio values of the pendulum vary at each different value and height of the load. Accordingly, in ZV input shaping method, pulse application amounts and times must change every time too. Otherwise, a good balance cannot be achieved each time. Therefore, in order to achieve the same success in different heights and weights other than training data, an NN based self-deciding control method is needed. The NN-based studies have also been reported in literature [6,14,16]. However, regression or radial-based NN methods have not been used in simple pendulum applications other than inverted pendulum [26–29]. The biggest advantage of these methods is that they can work with a small number of training data too. The single-layer NNs have been used to make performance comparisons of these methods. The missing success rates of these networks, trained with a small number of training data, have been tested to be maximized by using a serial connected second single layer NN, regression NN, and radial based NN methods. Here, NN + GRNN configuration provides the best performance.

Advantages of ZV input shaping method;

1- This is an open-loop controller and there is no need for the knowledge the system properties exactly.
2- For the detemination of input settings, it is sufficient to estimate the natural frequency and damping rate of the system.
3- ZV shaper is a forward compensator consisting of a series of impulses and it reaches the desired state without (/with minimum) the residual vibrations.
4- A ZV shaper is known for its a minimum time delay.
5- ZV shaper is a two-pulse method leading to the fastest system response.
6- With the ZV shaper, a system reaches the steady state quickly.
7- This technique is known to be the fastest method that shaper time length is the shortest.

Table 1a
Input shaping and hybrid control methods used in cranes.

	REF	YEAR	EXPERIMENTAL SETUP	MAIN METHOD	AUXILIARY METHOD	PURPOSES	BENEFITS
1	[6]	2012	Lab. Scale Gantry Crane	A NN Self Tuner Controller	ZV Shaper (For the Training Method)	Moving the load precisely and eliminate its swaying.	1. With this method, the controller can move the load with little oscillation. 2. Oscillation removal becomes evident over long distances.
2	[7]	2007	3D-Overhead Crane with Hoisting Mechanism	Adaptive Input Shaping Technique	ZV Input Shaper	Maximum suppression of the swings of the payload during both cart motion and the hoisting.	1. Parameters of shaper are constantly configured according to the linearized model and rope length.
3	[8]	2015	Double-Pendulum Bridge Crane	Input Shaping (ZV, ZV2M, ZV3M, SI2M)	Model Reference Control (MRC)	Asymptotic stability and reduce control effort.	1. IS-MRC increased the robustness of the vague distinction between the reference model and the plant. 2. IS-MRC can be designed for robustness of the plant.
4	[9]	2015	Double-Pendulum Tower Crane	ZV3M	MRC	Analyze and verify the robustness of the proposed controller in condition monitoring and oscillation suppression performances.	1. The robustness of the controller has been improved. 2. Perfect tracking performance and feasible control effort.
5	[10]	2015	Overhead Crane (Double-Pendulum-Type)	Fuzzy Control (SIRMs)	Simultaneous Input Shapers	Suppressing the motions of natural sway of payloads.	1. Combining input-shaping and SIRMs fuzzy control methods to analyze pendulum movements and transport control.
6	[11]	2008	30-Ton Bridge Crane	Input Shaping (ZV)	CMS Control	CMS was advanced for swing-free motion, disturbance rejection, precise positioning.	1. Oscillation reduction. 2. Disturbance rejection. 3. Positioning capability. 4. Payload oscillation detection. 5. Operator interface structure.
7	[12]	2002	Flexible Systems	Input Shaper	PDFeedback Controller	Limiting on overshoot, residual vibration, actuator effort with CEF controller.	1. Disturbance rejection. 2. Simultaneous feedback gains and input shaper design deliver higher levels of performance. 3. CEF is useful for overshoot and settling time.
8	[13]	2019	3D Overhead Lab. Crane	UMZV Shaper	PSO Algorithm	Efficient payload sway control despite crane hoisting effects.	1. Crane operators can cope with motion-induced sway problems. 2. The technique is effective during hoisting. 3. Optimal UMZV parameters are adjusted with PSO.
9	[14]	2018	Lab. Overhead Crane with Payload Hoisting	UMZV Shaper	ANN trained by PSO	Reducing the load swing of crane by hoisting and mass changes.	1. The proposed method can predict shaper's parameters. 2. According to ZVDD shaper it suppresses residual swing more.
10	[15]	2017	Lab. 3D Overhead Cranewith Friction.	PSO Algorithm	ZV and Distributed Zero Vibration (DZV)	Sway control of rail and trolley.	1. Effective load swing reduction achieved. 2. With the optimization process, input shaping parameters can be calculated without natural frequency and damping ratio.
11	[16]	2020	Overhead Crane	UMZV Shaper (NNUMZV)	AdaptiveFeedback Control (APIDLNN)	A new oscillation control approach for a crane despite payload hoisting and external disturbance.	1. The control parameters can be updated. 2. Suitable as an anti-swing controller in other cranes. 3. The method can handle payload hoisting and external disturbances.

Table 1b
Input shaping and hybrid control methods used in cranes.

	REF	YEAR	EXPERIMENTAL SETUP	MAIN METHOD	AUXILIARY METHOD	PURPOSES	BENEFITS
12	[17]	2019	Lab. Double-Pendulum Overhead Crane	MRCS	ATL-ZV and ATL-ZVD Shapers for Comparisons	Effective vibration and oscillation control.	1. MRCS is more robust towards changes in the frequency 2. The method can be beneficial for multimode flexible systems. 3. The MRCS is not robust to external disturbances.
13	[18]	2016	Lab-Scaled 3D Crane	PID + PSO	ZV Shaper	Fast and accurate positioning and minimum sway.	1. The method provides better position response with minimum sway. 2. It is robust to changes in different payloads and cable lengths.
14	[19]	2011	Multi-Mode Flexible Structure Systems	A Robust Input Shaping	SMOFC	Reducing the residual vibration although parameter uncertainties and external disturbances.	1. The stability of closed-loop system is guaranteed in case of unknown upper bounds on norm of uncertainties.
15	[20]	2017	Overhead Crane	ZV, ZVD Shaper	FM Feedback	Elimination of residual oscillations.	1. Frequency modulation is used to tune the system frequency. 2. Partial feedback linearization is used to eliminate the time-dependent damping of the system. 3. A major advantage is the flexibility in changing the hoisting cable length without restrictions. 4. Residual oscillations using the FM shaper are not affected by the maneuver trajectory.
16	[21]	2017	Double-Pendulum Bridge Cranes	Combined Input Shaping	Feedback Controller	Effectively rejection of external disturbances and ensuring quick point-to-point motion.	1. The method obtains quick point-to-point response alike to open-loop input-shaping control. 2. It minimizes transient deflections 3. The method effectively suppresses the disturbances and is robust to modelling uncertainties.
17	[22]	2013	Gantry Crane	Hybrid Input Shaping	PID Controller	Active sway control.	1. The hybrid input-shaping and PID guarantee a quick input tracking, precise payload positioning and minimal sway.
18	[23]	2009	Gantry Crane	PD-Type Fuzzy Logic	Hybrid Input Shaping	Cart position and anti-swaying control.	1. The methods can reduce oscillation angle while protecting the input tracking performance. 2. A slower trolley trajectory response with less overshoot was achieved with ZSDD when compared with PD-type FLC.
19	[24]	2012	Flexible Structures	Input Shaping	Adaptive SMC	Reducing or eliminating residual vibration.	1. The stability of closed-loop system is guaranteed. 2. This method ensure closed-loop system stability, and yields well performance, robustness of parameter uncertainties, external disturbances as well. 3. Increasing the robustness to parameter uncertainties does not lengthen the duration of the impulse sequence.
20	[25]	2017	Mass-Damper-Spring Plant	Input Shaping (ZV and ZVD)	Quantitative Feedforward-Feedback Controller	Minimal residual vibration.	1. Input shaper reduces vibration from reference input, while quantitative feedforward-feedback controller reduces vibrations from disturbances and noise. 2. The proposed technique is simple enough to be applied to complicated plants.

3. Material and methods

3.1. Material

In this study, Makeblock mechanical fittings were used for the simple pendulum mechanic construction. Other pieces of equipment are Pololu 12 V brushed DC motor with integrated 48 CPR quadrature encoder (2250 RPM, 300 mA free-run, 5.6 A stall) [30], Pololu simple high-power motor controller card 24V23A [31], Yumo rotary encoder – 200P/R (Quadrature) [32], Humusoft MF 634 multi-function I/O data acquisition card for PCI Express [33], Globex GXA1216 power source (12 V, 16.7 A) and fully equipped computer (Windows 7, 64 bit, Intel Core i5-7500, 3.40 GHz, 16384 MB ram memory, AMD Radeon R7200 series graphics processor). The system was integrated with the Matlab/Simulink environment. Fig. 1 shows the details of the experimental setup indicating that the simple pendulum is very much similar to a gantry crane. The Gantry cranes are like bridge cranes. The only difference is that they are mobile and operate on a runway on the near floor and stand on at two pairs of steel legs. Generally, they are used in shipyards, factories, storehouses [34].

Table 2a
Method comparisons.

	REF	YEAR	COMPARISONS AND SUCCESS RATES
1	[6]	2012	1. Effective reduction in load swing 2. More convenient for longer roads according to a PID with constant gain 3. According to standard input shapers, more robust to change of cable length and length uncertainty with use of feedback.
2	[7]	2007	1. The controller efficacy is more than according to standard shapers for time-varying systems. 2. The oscillations occurring in the load during the maneuver are greatly reduced with the adaptive input shaper, in comparison with the standard shaping technique.
3	[8]	2015	1. The SI2M-MRC is more robust than the IS-MRC about plant uncertainties. Because load and hook swings are better suppressed. 2. SI2M shaper suppresses both modes of oscillation below 5%.
4	[9]	2015	1. The controller has good robustness in terms of system difference between parameter and reference plant and parameter estimation errors. 2. On robustness analysis, the ZV3M-MRC does a good job on oscillation reduction and state tracking. 3. The hook and payload oscillations (About ± 0.24° in the residual swing) were effectively suppressed. 4. The method reduces the load max residual swing between 0.10°~0.36°.
5	[10]	2015	1. Compared three control methods; SIRMs fuzzy controller, the convolved input-shaping-based (CIS) SIRMs and (SIS) SIRMs fuzzy controllers. 2. Simultaneous input-shaping-based SIRMs fuzzy method is faster than the convolved input-shaping based SIRMs fuzzy method. 3. The (SIS) SIRMs fuzzy method has minimum residual oscillations.
6	[11]	2008	1. Motion-induced hook oscillations were reduced about 90%. 2. The control can reject externally induced hook oscillation and positioning of the hook is a few centimeters. 3. Operators using the visual interface complete positioning tasks 5% to 45% faster than manual control.
7	[12]	2002	1. Input shaping PD feedback control is more successful than PD control. 2. Performance is optimized simultaneously thanks to feedback gains and input shaper design. 3. Although the performances of Input shaping PD controller and CEF controller are close, the CEF system moves faster.
8	[13]	2019	1. With the proposed shaper substantial sway reductions were achieved in both hoisting cases. 2. According to ordinary techniques, there was at least a two-fold reduction in maximum transient and residual oscillations. 3. With this technique choosing the shaper parameters was achieved automatically during the hoisting operation.
9	[14]	2018	1. With this method, at least 38.9% and 91.3% reductions in total and residual oscillation responses were achieved via a UMZV. An average operating frequency and ZVDD was used for this. 2. ANN-UMZV can estimate and update shaper parameters and has the advantage of shorter shaping time and faster response. 3. ANN-UMZV, AOF-UMZV and ZVDD shapers were capable to suppress the induced swing angle at least by 90.74% and 89.81% reductions for the 0.74 kg and 0.24 kg, respectively. Comparison made according to unshaped response. But ANN-UMZV was very good about MSE and RS values.
10	[15]	2017	1. PSO-based ZV and DZV input shapers with nonlinear model were compared with analytical-based input shapers that using a linear second order model for sway control. 2. Both shapers provided higher sway reductions. 3. 30–50% reductions of the IAE values were obtained with PSO-based ZV and DZV input shapers according to analytical-based input shapers.
11	[16]	2020	1. Though all conditions the improved controller achieved minimum 45% and 69% oscillation reductions in overall and residual oscillation responses, according to a comparative method. 2. The proposed controller is more succesfull than NNUMZV-PIDPSO controller. 3. Test conditions contain three experimental cases with payload hoisting, a non-zero initial condition, persistent (wind) and instant disturbances. 4. According to MSE values about overall swing response improvements of 86%, 45% and 87% were achieved according to the NNUMZV PIDPSO method for cases 1, 2 and 3 respectively. 5. According to comparative method Anti-swing control with improvements is at least by 69%. Also nearly there is no residual swing.
12	[17]	2019	1. Simulations and experiments were carried out under two situations, without and with load hoisting, and with different loads. 2. Without knowing system frequency and damping ratio values MRCS provided the highest reductions according to the multimode ATL-ZV and ATL-ZVD shapers about overall hook and load swings based on the Average Travel Length approach. 3. The MRCS provided 31.8%, 2.5% and 24%, 2.6% reductions in the overall hook swings and 66%, 2% and 61.8%, 20.5% reductions in the load swings according to the multimode ZV, ATL-ZV and ZVD, ATL-ZVD shapers respectively. 4. MRCS was better in the swings reductions than the robust multimode ATL-ZVD shaper.
13	[18]	2016	1. The suggested method is better than PID-PID + PSO anti oscillation method. 2. The proposed controller can not handle environmental disturbances. 3. While the PID-PID controller needs an extra sensor the proposed scheme do not need any angular sensor to measure the sway angle. 4. The suggested controller shows no over shoot in both directions of the crane about position response and it has lower IAE values (20% and 10% for rail and trolley respectively) and faster settling time is about half of PID-PID controller. 5. With the optimal PID and PID–PID controllers, max. transient sways are 5°, 4° and 7.5°, 5.5° degrees and at the simulations, these angles are 4.5°, 4.2° and 5°, 6.1° degrees for rail and trolley respectively. 6. Optimal PID controller provides slightly higher residual about oscillation of rail that negligible. But less residual oscillation of the cart response is seen.
14	[19]	2011	1. SMC has some good properties. Quick response, well transient performance, insensitiveness to the parameter uncertainties and external disturbances. It has a good trajectory tracking though parameter uncertainties. 2. SMOFC do not add any additional dynamics and is easy to apply.
15	[20]	2017	1. Occasionally hoisting speed can change during the input shaping application. A minor drift in jib's position is seen so an additional modified FM input shaping application is used. 2. The FM is added to the unshaped travel command. The aim is remove any waste speed. 3. The modified FM shaping removes restrictions on hoisting process. 4. With this scheme there is important reduced sensitivity of the FM + ZVD shaper according to the traditional ZVD shaper. 5. The system is very tolerant to cable length reading mistakes. 6. ZV shaper has ± 10% offset tolerance, ZVD shaper has ± 17% values.

3.1.1. Control block

So far, a lot of studies have been done on hybrid control techniques. The purpose of all these studies is achieving precise cart positioning and low payload oscillations, simultaneously [34]. In this study, it is aimed at controlling a simple pendulum under variable loads and heights by using the ZV-IS and ANN methods. The category of Probabilistic Neural Networks (PNN) can be trained with only a fraction of the training samples [35]. Usually, data obtained from the operating system is not enough for a backpropagation NN. So for the PNN, a few training samples are enough to converge to the basic function of data. For these advantages, a hybrid control method was developed. Single-layer NN and PNNs were used together. Five hun-

Table 2b
Method comparisons.

	REF	YEAR	COMPARISONS AND SUCCESS RATES
16	[21]	2017	1. The controller is robust about system parameters. For example mass ratio, move distance, and modelling uncertainties. 2. For practical applications the aim is high effectiveness in suppressing residual swing and keep the duration of the shaper minimum. 3. The final shaper design has less than 8% relative oscillation for changes in mass (-90% and + 110%.). So the EI shaper is robust to significant modelling uncertainties. 4. The combined controller crucially increases performance. It exhibits average 60% reduced transient oscillation and decreases settling time by 3 s. 5. For all the cases the maximum payload deflection varied for shortest and longest command duration between 0.27° and 10.3° degrees.
17	[22]	2013	1. The hybrid PID controller and input shapings with higher number of impulses ensure a high level of oscillation reduction. 2. Oscillation reduction of PZSDD, PZSD and PZS are ± 0.0358 rad, ± 0.0081 rad and ± 0.0039 rad respectively. 3. In Input shaping, a slower response occurs as the impulse increases. In none of these methods there is a surge in cart movement responses. 4. PZSDD PID controller has highest level of oscillation reduction.
18	[23]	2009	1. The hybrid control schemes are created with PD-type FLC and feedforward control using the ZS and ZSDD shapers. 2. The PD-type FLC with ZSDD shaper provides better level of swing angle reduction. 3. ZSDD shaper results in a slower tracking response with less overshoot about speed of the responses. 4. The PD-type FLC with ZS shaper results in a faster rise time and the settling time of the trolley trajectory response is faster than the PD type FLC with ZSDD shaper.
19	[24]	2012	1. Here is the purpose, preparing a closed loop input shaping scheme based on adaptive SMC. It will behave as the reference model with input shaper and completely eliminate the residual oscillation despite of parameter uncertainties and external forces. 2. This technique has a good oscillation reduction and robustness properties despite of both parameter variations and the resonant external forces.
20	[25]	2017	1. The feedforward-feedback (FF) system overcomes the indefiniteness, external disturbances and noise. 2. This method is less conservative than the pure-feedback system and can resist large plant ambiguity with fast move time when compared with traditional robust shaper. 3. The FF controller is less conservative so has less cost of feedback than the feedback-only controller. 4. The FF system has less gain than the other system but delivers equally good performance. This less gain reduces the control effort used and avoids more noise at high frequencies. 5. The tracking performance of the FF system is a little better than other system. 6. Both systems are more robustness about model uncertainty and smaller settling time and they superier than ZV and ZVD shapers. 7. The FF system utilizes feedback to reduce oscillations induced by disturbance and noise and provides well robustness to plant model uncertainty.

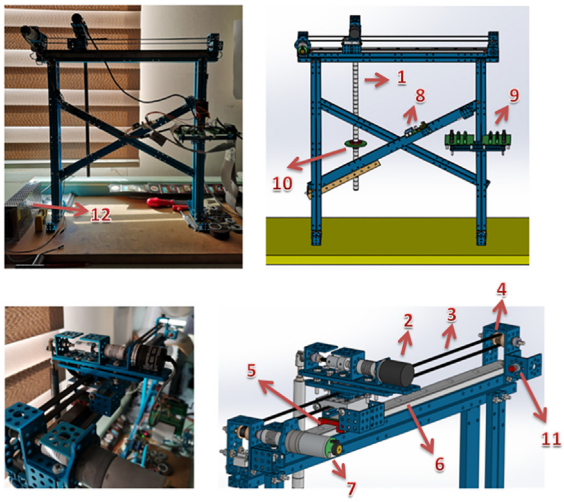


Fig. 1. Simple pendulum: 1-Pendulum bar, 2- Encoder, 3- Belt, 4- Pulley, 5- Trolley, 6- Mono-rail, 7- DC motor, 8- Motor controller card, 9- Data acquisition card slots, 10- Variable weights, 11- Stopper, 12- Power supply.

dred twenty-eight lines of input data was enough to perform a comparison of GRNN, RBFN and second single-layer NN. An eleven analog input and six analog output values are used during training. These analog outputs are, t_1 and t_2 pulse times, V_1 and V_2 the speed values required for the most appropriate amplitude amounts and the application times t_{appt1} and t_{appt2} required to meet these amplitude amounts. t_1 and t_2 are the pulse times which determine the start time of amplitudes. The analog inputs are period (T), damping ratio (ζ), weight (m), load position (h), damped natural frequency (W_d), natural frequency (W_n), damping constant (c), spring constant (k), amplitude parameter (K) and Posicast input amplitudes (A_1, A_2). In addition, for NN training of V_1, V_2, t_{appt1} and t_{appt2} values they are separated from the others. This is due to the fact that if one trains using these four values at the one Simulink block, some of them will have low training success rates because of lack of necessary input training data lengths.

It is decided to train output analog values separately at the first NN Simulink blocks. In this case, t_{appt1} and t_{appt2} application times values are very crucial. If there is not enough training ratio for this application times, It can not achieve the pen-

dulum rod balance for the ZV-IS control method. This decision made it possible to train a high rate of all data. Firstly, single-layer NN blocks were used as a first intelligent controller block. Then, the missing aspects of first NN blocks is fixed with second NN blocks. Some trials were made for second cycle trainings with other intelligent controller methods such as second single-layer NN, GRNN Function Approximation, Radial Basis Approximation Neurons (RBAN), Radial Basis Underlapping Neurons (RBUN) and Radial Basis Overlapping Neurons (RBON).

These control blocks were connected in series one by one. Because of this form, firstly there are only eleven analog inputs and one analog output for the first NN blocks. If you have insufficient data at the first NN blocks'output values you can obtain more accurate values by the second data training NN blocks' output without sensors or other control types of equipment data. For this reason, second data training blocks have only one analog input values so will have only one analog output values as shown in Fig. 2. This structure is an OL control method. There is no return notification necessary for error values owing to NN control blocks in the second stage. In this way, the load positioning has been carried out successfully by two pulsed ZV-IS method at an arbitrary time gap. The same success was achieved in different weights and heights except for the training weights and heights. As seen in Fig. 2, there are four pieces of retard blocks at the end of the intelligent controller group. It was noticed during the studies that, especially when we were working with the second stage NN blocks, a momentary hold of the four analog output values gave more accurate test results. According to many studies, the amount of this delay time is not critical. Therefore 0.01 s during the training and 2 s during the testing was selected. These values were determined as arbitrarily.

3.2. The methods

3.2.1. ZV input shaping

The input shaping (IS) technique is an OL control method. In fact, the IS technique is an auxiliary control technique and mainly designed for systems like bridge cranes [2,4,36]. In the experiments, it was seen that the operators use the cranes faster, safer and more effectively with this technique [4]. Moreover, a zero over travel IS was thought up to decrease overshoot in a crane [36]. In [2], the IS controller was more successful than the PD-control according to analysis. The lower the mean finishing time and the less energy depletion that led to this difference. This performance has also been investigated in double pendulum bridge cranes [37–40]. As a result, experimental studies have also shown that operators use cranes faster and safer. If you want to think up an IS-Cr (Controller), you must estimate the system's natural frequency and damping ratio. [41]. But, real systems can not be modeled very well. For that reason achieving the robustness to modeling errors is significant. Generally, the robust shapers use more time and system response is slower. Together work of shaper duration and robustness analyzed that Extra Insensitive Shaping (EI-S) technique performed better than other methods (ZV, ZVD, ZVDD) according to theoretical results. A review of CmS (Command shaping) techniques for flexible connection manipulators has been made too [42]. This study presented command pre-shaping methods. The compromise of the quickness of movement and shaper robustness was investigated using 15 different IS methods. These methods are smoothly shaped reference commands and all positive input shapers reported in the literature. On the other hand, a benchmark table was provided. The

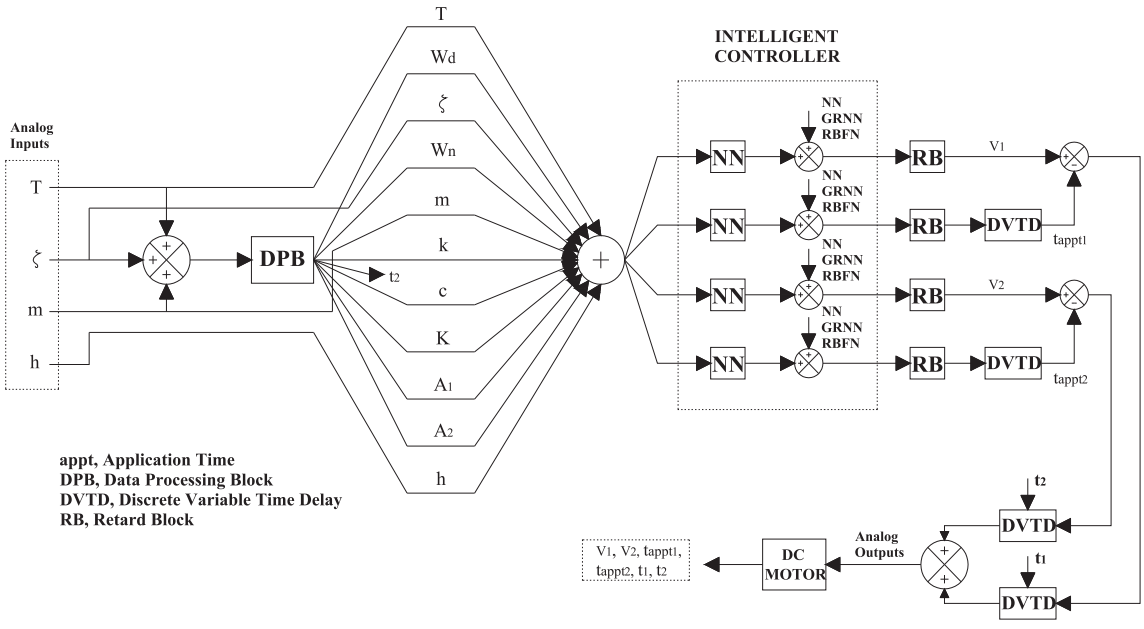


Fig. 2. Input shaping positioning control block.

methods were listed according to insensitivity. Consequently, the presented review paper ensures to cover most of the details for the IS methods in the literature.

3.2.2. Single-layer ANN

The ANN techniques have the ability to produce solutions to many problems. They are defined in different ways and related definitions have a few common points. At the very beginning, the ANNs are composed of artificial cells that can be connected to each other hierarchically and they operate in parallel. It is assumed that these cells, also called process elements, are connected together and each link has value. The common point is that information is obtained through learning and the process elements are stored at the connection values, and they have a distributed memory. The network formed as a result of connecting the process elements with each other is called an ANN. The creation of this network is based on findings of the biological nervous system [43].

Single-layer ANNs only consist of input and output layers. Each network has one or more inputs and outputs (C). Output units are connected to all input units (X). Each connection has a weight (W). There is a threshold amount (Φ). It prevents the output of the network to be zero. The input of the threshold amount is always one. The output is calculated by summing the weighted input amounts with the threshold amount. This input value is passed through an activation function so the networks' output is figured out [43]. This is formulated as follows;

$$C = f(\sum_{i=1}^{m} W_i X_i + \Phi) \tag{3.1}$$

In single-layer NNs, the output function is linear. In other words, the examples shown on the network are divided between two classes and a straight line. The threshold function is used for determination of the output. Here the output of the network is 1 or -1. 1 and -1 represent classes. If the output of the network is 1, in the first class, -1 it is accepted in the second class. If considers in Fig. 3, it is a straight line that separates the two classes [43].

This straight line, also called the class separator, is defined as follows [43];

$$W_1.X_1 + W_2.X_2 + \Phi = 0 \tag{3.2}$$

From here,

$$X_2 = -\left(\frac{W_1}{W_2}\right).X_1 - \Phi/W_2 \tag{3.3}$$

$$X_1 = -\left(\frac{W_2}{W_1}\right).X_2 - \Phi/W_1 \tag{3.4}$$

From these two formulas, the class separator can be drawn as in Fig. 3. The purpose of learning in these networks is to specify the position of the class separator line in a way that best distinguishes both groups. For this, the weight values need to be changed. That is if the time values in the time unit t are changed as much as ΔW;

$$W_i(t+1) = W_i(t) + \Delta W_i(t) \tag{3.5}$$

During learning, this change is carried out in each iteration to find the correct position of the class separator. Changing the weight means changing the slope of the line. This may not be enough. The threshold value must also be changed. This helps to shift the line between classes. Thus, the position of the activation function is determined. In this instance, the threshold value at time t is changed as undermentioned [43].

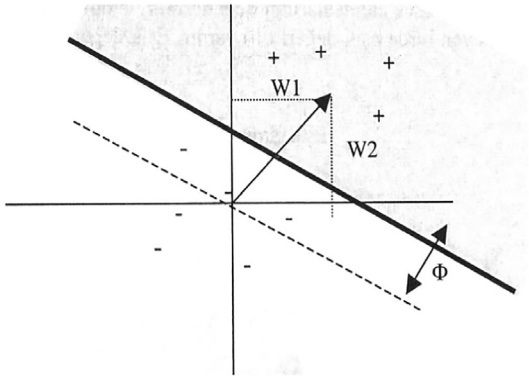


Fig. 3. Geometrical representation of weights and the straight line being the class separator.

$$\Phi(t+1) = \Phi(t) + \Delta\Phi(t) \tag{3.6}$$

During learning, the threshold value is changed in each iteration as much as $\Delta\Phi$ as in weights [43].

3.2.3. GRNN

A GRNN is the most suitable NN for function approximation for the purpose. The GRNN is a kind of RBF-NN with one-time learning [44]. Also, it was presented by Donald F. Specht in 1991 [45] and based on the Nadaraya-Watson Kernel [46]. GRNN is suitable for many applications. Such as; geographic modeling, image inpainting and restoration, predicting the change in length of the day, prediction of scour depth, health index calculation of power transformers, exhaust emissions in HCCI engine, signature recognition, diagnosing thyroid disease [47–54]. According to the studies, the GRNN method has obtained more successful results than other methods [46–54].

Fast learning and convergency to the optimum recession surface according to the number of samples, are the primary advantages of GRNN. The GRNN is favorable with rare data in real-time surroundings. The reason for this is immediately described everywhere even a single sample is enough. No additional input is required by the user [45]. This makes GRNN very beneficial for performance forecasts and comparisons [35]. The GRNN method is more suitable for the functional approach [47].

The GRNN structures are also applicable to classification problems [46,47,50]. GRNN is a FF (Feedforward) network based on the probability density function. There are four layers in this network structure as in Fig. 4 [55]. These are the input, pattern, summation and output layers [45]. The number of input neurons (Nrs) depends on the number of problems input as in other networks. The number of intermediate layers (Pattern Layer) is the number of samples. The number of Nrs in the col-

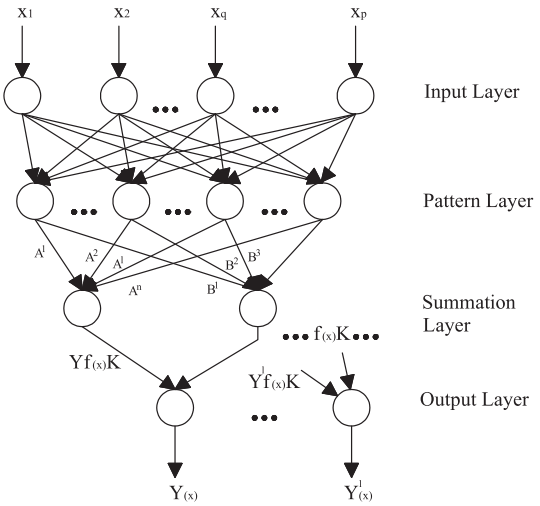


Fig. 4. GRNN structure.

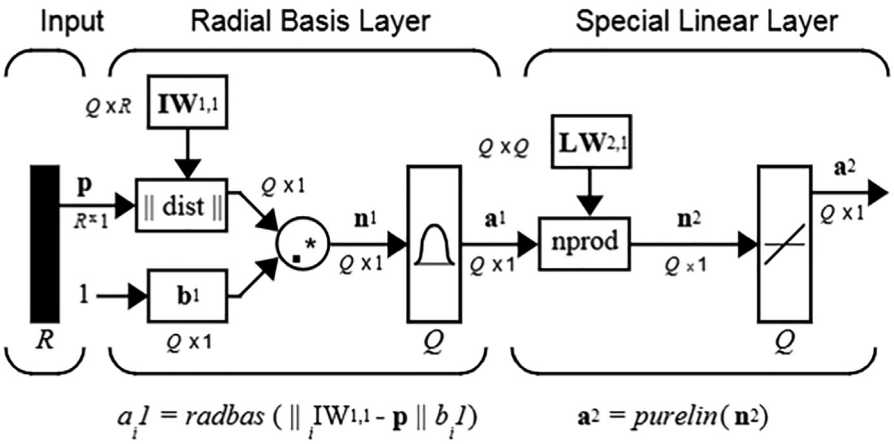


Fig. 5. GRNN network architecture.

lection (Summation Layer) floor is more than the number of outputs [55]. The layer structure of GRNN is demonstrated in Fig. 5. It is the same as the RBN except for the second layer due to some differences [56].

In GRNN solely smoothing parameter (σ) is upgraded [46,57]. The σ values are significant; smaller σ restraints the amount of efficient samples, also, the wider one enlarges the radius of efficient neighbors [47,52]. During programming, the user chooses a *spread* value. The meaning of a broader *spread* is causing more space around the input vector. In that place layer 1 Nrs will responces with important outputs. Thus if the *spread* is small the RBF is complete perpendicular in this way the Nr that having the weight vector nearest to the inlet will have a much larger output than other Nrs. The network has the tendency to respond with the target vector [58]. If *spread* gets larger, the RBF's slope gets straight. Also, a lot of Nrs may respond to an input vector, then the network takes a weighted mean. It takes this mean between target vectors. In here, design input vectors are nearest to the new input vector. When *spread* gets larger with more Nrs the network function gets straight [58]. Unlike backpropagation NNs, GRNN requires only a part of training examples like other probabilistic NNs [45]. Data measurements obtained from an operating system are never enough for a backpropagation NN [59]. So probabilistic NNs are favorable about the ability to converge to the basic function of the data with a few training examples [35]. Also, GRNN is a good alternative for the solution of regression, approximation, classification and fitting troubles [60]. It can also be employed to identify and control of dynamic systems. The GRNN has shorter training time and higher accuracy than the counterpart back-propagation NNs according to comparisons. The GRNN controller performance is greater than 95% or almost nearly 99%. In [26], a balancing control was developed for control purposes. The GRNN-Cr can hold the biped in the upright direction as an inverted pendulum. Meanwhile, there are some restrictions on GRNN, such as expansion of the hidden layer. When you train a GRNN with lots of data, it is important to decrease the data dimensionality using any of the data reduction methods for example clustering or distance based algorithms [60]. Also to achieve the most suitable performance, the *spread* value must adjusted to have a value between 0 and 1. If you have a smaller number about the *spread,* it will give you a best-fit approximation. If you have a higher value about *spread,* this time it will give you a smooth performance of approximation [61].

3.2.4. RBFN

It is one of the ANN structures used in multivariate modeling and convergence. The processor elements in the intermediate layer do not employ the weighted form of the inputs and the outputs of the processor elements in the intermediate layer adjusted according to the length between the ANN inputs and the centric of the primary function. The RBFN structure includes intermediate layer processor elements that are radially symmetrical in its most general sense. The intermediate layer processor element output is only a function of the length between the center, the input vector and is one of the ANN structures used in multivariate interpolation approaches. The processor elements in the initial layer don't make use of the weighted form of the inputs. The outputs of the processor elements in the first layer are defined by the length among the ANN inputs and the centric of the main function. The last layer of radial based (RBF / RBFN) ANN structures are linear and produce a weighted total output from the outputs of the first layer. The RBFN commonly used in practice has been proposed by Moody and Darken [62]. Similar algorithms have been investigated by researchers such as Powell [63], Broomhead and Lowe [64] who work on interpolation and convergence problems. This network architecture is given in Fig. 6. Here, the interlayer processor elements are completely connected to an output layer of linear structure. The output of the processor elements can be obtained as this [55];

$$I_k = \| X - c_k \| = \sqrt{\sum_{i=1}^{N} (X_i - c_{ki})^2}, k = 1, 2, ..., N \tag{3.7}$$

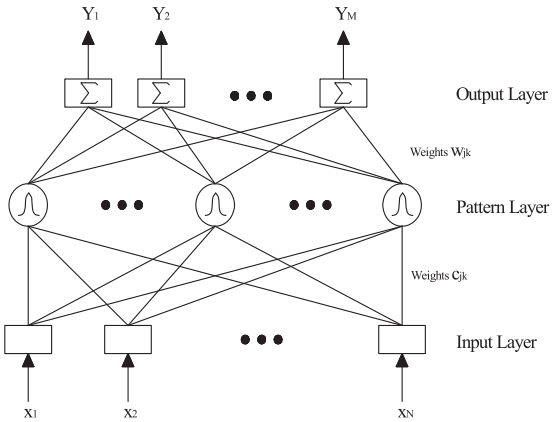


Fig. 6. RBFN structure.

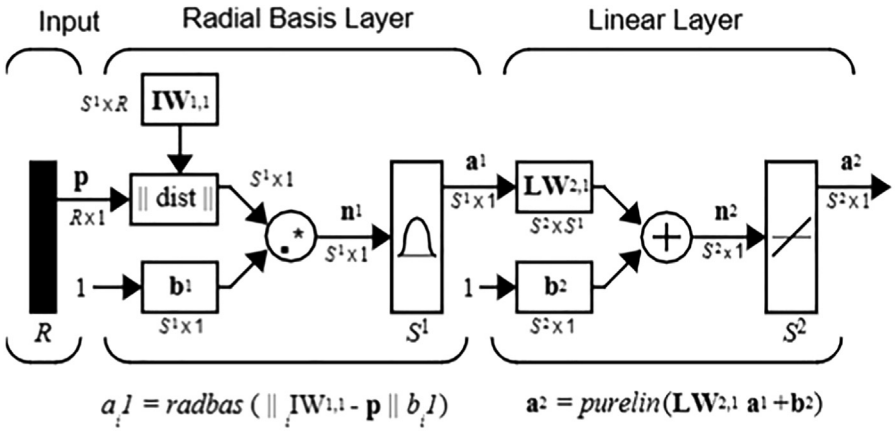


Fig. 7. RBFN network architecture.

If neuron (Nr) output,

$$v_k = e^{-\frac{l_k}{\sigma_k^2}} \tag{3.8}$$

X is the multidimensional input vector, c is the centric vector of the equal size with the input vector, and σ is the classic deflection value. The c_k weights and σ_k widths must be determined to train the intermediate processing elements.

In classification, Multilayered Perceptrons (MLP) structures create classes using intermediate layer processor elements that create hyperplanes in the data space, while RBFN structures model separate class distributions as if using native kernel functions. To classify these classes, a kernel function is placed in hyper-surfaces or in each class. RBFN learns structures faster than MLP networks. However, with increasing input, very high dimensional RBFN structures are needed. These structures are often used to resolve problems for instance system modeling, prediction, and classification. The RBNs comprise two layers as in Fig. 7. A hidden RB layer of S^1 Nrs and an output linear layer of S^2 Nrs [56]. The *spread* factor parameter is important in RBFN performance. The meaning of a larger *spread* has a big area on all sides of the input vector. In there layer 1 Nrs will answer with important outputs. For that reason, while the *spread* is small the RBF is very perpendicular. Thus the Nr that has a weight vector nearest to the input will have a more extensive output than other Nrs. The network inclines respond with the target vector related to the closest design input vector. When *spread* gets larger the RBF's slope gets smoother. Also, several Nrs may respond to an input vector. The network after pretends as it is taking a weighted mean among target vectors. Likewise, design input vectors are nearest to the new input vector. As *spread* gets more Nrs, the network function becomes smoother [58].

Besides these, designing and analyzing a precise dynamic model for the overhead crane is a critical step. For this MCS was used to optimize the RBF-NN models in [65]. The aim was modeling the overhead crane system and accomplished it with great precision. Also, a novel MPC scheme was presented in [27]. The proposed approach utilized from a robust inverse RBF model. The controller performance has been evaluated with an inverted pendulum on a trolley. As a result, the calculation time was reduced. In the other study, the inverted pendulum test setup was used for the learning performance of FACRLN based on a Fuzzy RBF in [28]. The aim of this control structure was the training of the FACRLN for balancing the pole. On the other hand, the PSO-based RBFNs system was improved in [29]. According to simulation results, RBFNs' efficiency on the inverted pendulum was shown.

Underlapping Nrs (RBUN); The *spread* of the RB Nrs is very low, the network needs more Nrs to comply with a smooth function and the network might not universalize very good. Such as; *spread* = 0.01.

Overlapping Nrs (RBON); The *spread* of the RB Nrs is very high, each Nr responds fundamentally to the similar. Many Nrs are necessary to fit a rapid replacement function. Such as; *spread* = 100

Approximation Nrs (RBAN); The larger *spread* is, the smoother the function approximation. Such as; *spread* = 1

As a result, not choosing a very complex model and good training error performance does not bring the same rate of testing performance [66].

4. Experiment studies

4.1. First stage of neural networks

So far, a lot of investigation has been done on hybrid control techniques. The purpose of all these studies is achieving precise cart positioning and low payload oscillations, simultaneously [34]. In this study, it is aimed to control a simple pendulum under variable load and height by using the ZV-IS method and ANN methods. For this purpose, a single-layer NN was used with second single-layer NN, GRNN, and RBFN. This control mechanism was operated in series with each other. In this

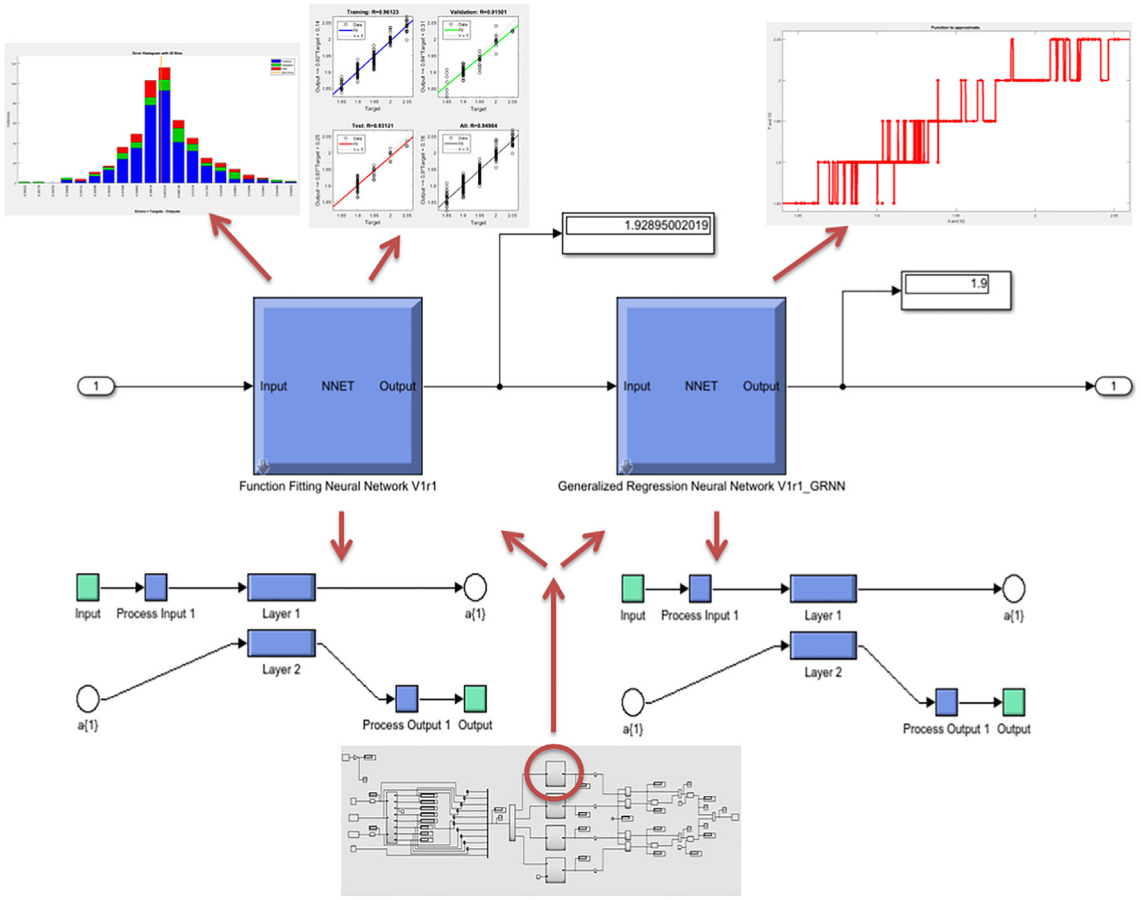


Fig. 8. Neural network control blocks.

way, the load positioning has been carried out successfully by two pulsed IS method at an arbitrary distance. The same success was achieved in different weights and heights except for the training weights and heights.

As shown in Fig. 8, a function fitting NN block and the GRNN block are positioned in series. The errors in the first block were eliminated in the second block exit and the desired values were obtained eventually. If you look at the first output of NN blocks, numbers have decimal points in Fig. 8. The digits of these numbers range from 11 to 14. These different numbers becomes very useful in the second training phase. The function to approximate block is seen in Fig. 8 in the right upper corner. The values which are far from the mainline rising in the form of steps are brought to the values that should be on the mainline. The number of data entering the first NN block is eleven and the number of output data is one.

In the second GRNN block, one data is entered and one data is output. The same application logic is also seen in NN + RBFN. This application was done in the Simulink environment by Matlab. Also, the same hybrid application was done to find V_2,t_{appt1} and t_{appt2} values with V_1. Fig. 10(a) shows that there are thirty-one test points on the pendulum bar. These test points were placed at 11.66 mm intervals. These are; 0, 1, 11.66, 23.33, 35, 46.66, 58.33, 70, 81.66, 93.33, 105, 116.66, 128.33, 140, 151.66, 163.33, 175, 186.66, 198.33, 210, 221.66, 233.33, 245, 256.66, 268.33, 280, 291.66, 303.33, 315, 326.66, 338.33, 350 mm. The pendulum's bar weight is 370 g. The training weights are; 8, 16, 21, 29, 37, 42, 50, 58, 63, 71, 79, 84, 92, 100, 105, 113, 121 g. As a result seventeen (Except Pendulum's Bar Loadless Weight) different weights were used so a total of 528 (31x17 = 527 + 1(Loadless) = 528) training data line were performed. With all these numbers, first single-layer NNs were trained for a 200 mm moving distance as in Table 3.

Thus, the first phase of the NNs training was completed. While training NNs, Matlab/Simulink, Neural Fitting (nftool) Toolbox was used. The training algorithm was Levenberg-Marquardt. NN's weight and threshold values are produced by the toolbox and for that reason, you can not interfere. The velocity values of V_1 and V_2 relative to the analog signal values are shown in Fig. 9. 56.25% percent of the DC motor speed capacity was used in this study.

4.2. Second stage of neural networks

Different decimal numbers that come from the first stage NN blocks were used for training of second single-layer NNs, GRNNs, and RBFNs.

Table 3
First stage NNs training data and results.

For the V_1 value, NN training Nrs number was 15 at the hidden layer and training algorithm was Levenberg-Marquardt. 528 lines of data; 70% (370) was for training, 15% (79) was for validation and 15% (79) was for testing. Regression values were; Training: R = 0.97549, Validation: R = 0.93243, Test: R = 0.8976, All: R = 0.95532. Epoch value was 86 iterations and performance values were MSE = $1.87575e^{-4}$, R = $9.55315e^{-1}$. Five different analog signal values were used to optimal V_1 speed value during training. These were; 1.85, 1.90, 1.95, 2.00, 2.05.	For the V_2 value, NN training Nrs number was 20 at the hidden layer and training algorithm was Levenberg-Marquardt. 528 lines of data; 70% (370) was for training, 15% (79) was for validation and 15% (79) was for testing. Regression values were; Training: R = 0.96888, Validation: R = 0.90889, Test: R = 0.91276, All: R = 0.94956. Epoch value was 60 iterations and performance values were MSE = $2.52779e^{-4}$, R = $9.49563e^{-1}$. Five different analog signal values were used to optimal V_2 speed value during training. These were; 1.70, 1.75, 1.80, 1.85, 2.00.
For the t_{appt1} value, NN training Nrs number was 10 at the hidden layer and training algorithm was Levenberg-Marquardt. 528 lines of data; 70% (370) was for training, 15% (79) was for validation and 15% (79) was for testing. Regression values were; Training: R = 0.99909, Validation: R = 0.99911, Test: R = 0.99834, All: R = 0.99897. Epoch value was 21 iterations and performance values were MSE = $9.14452e^{-9}$, R = $9.98974e^{-1}$. Three different analog signal values were used to optimal t_{appt1} time value during training. These were; 0.400, 0.401, 0.405.	For the t_{appt2} value, NN training Nrs number was 10 at the hidden layer and training algorithm was Levenberg-Marquardt. 528 lines of data; 70% (370) was so as to training, 15% (79) was for validation and 15% (79) was for testing. Regression values were; Training: R = 1.0, Validation: R = 1.0, Test: R = 1.0, All: R = 1.0. Epoch value was 40 iterations and performance values were MSE = $1.13642e^{-11}$, R = $9.99999e^{-1}$. Two different analog signal values were used to optimal t_{appt2} time value during training. These were; 0.940 and 0.950. (t_{appt2} = $t_{appt2total}$-t_2)

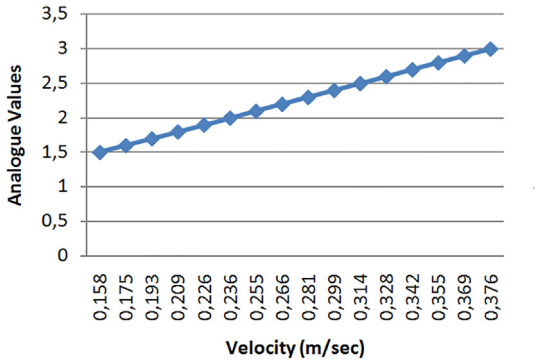


Fig. 9. DC motor speed values.

Table 4
Second stage NNs training data and results.

For the V_1 value of second single-layer NN training Nrs number was 30 at the hidden layer and training algorithm was Levenberg-Marquardt. 528 lines of data; 70% (370) was for training, 15% (79) was for validation and 15% (79) was for testing. Regression values were; Training: R = 0.97061, Validation: R = 0.97632, Test: R = 0.9795, All: R = 0.97257. Epoch value was 90 iterations and performance values were MSE = $1.16404e^{-4}$, R = $9.72565e^{-1}$. Five different analog signal values were used to optimal V_1 speed value during training. These were; 1.85,1.90,1.95,2.00,2.05.	For the V_2 value, NN training Nrs number was 35 at the hidden layer and training algorithm was Levenberg-Marquardt. 528 lines of data; 70% (370) was for training, 15% (79) was for validation and 15% (79) was for testing. Regression values were; Training: R = 0.96027, Validation: R = 0.98044, Test: R = 0.93481, All: R = 0.95996. Epoch value was 10 iterations and performance values were MSE = $1.99798e^{-4}$, R = $9.59964e^{-1}$. Five different analog signal values were used to optimal V_2 speed value during training. These were; 1.70, 1.75, 1.80, 1.85, 2.00.
For the t_{appt1} value, NN training Nrs number was 15 at the hidden layer and training algorithm was Levenberg-Marquardt. 528 lines of data; 70% (370) was for training, 15% (79) was for validation and 15% (79) was for testing. Regression values were; Training: R = 0.99993, Validation: R = 0.99989, Test: R = 0.99981, All: R = 0.99991. Epoch value was 8 iterations and performance values were MSE = $8.17182e^{-10}$, R = $9.99907e^{-1}$. Three different analog signal values were used to optimal t_{appt1} time value during training. These were; 0.400, 0.401, 0.405.	For the t_{appt2} value, NN training Nrs number was 5 at the hidden layer and training algorithm was Levenberg-Marquardt. 528 lines of data; 70% (370) was so as to training, 15% (79) was for validation and 15% (79) was for testing. Regression values were; Training: R = 1.0, Validation: R = 1.0, Test: R = 1.0, All: R = 1.0. Epoch value was 40 iterations and performance values were MSE = $8.42989e^{-12}$, R = $9.99999e^{-1}$. Two different analog signal values were used to optimal t_{appt2} time value during training. These were; 0.940 and 0.950. (t_{appt2} = $t_{appt2total}$-t_2)

4.2.1. Single-layer neural network (NN)

Second stage NNs training data and results are shown in Table 4.

4.2.2. General regression neural network (GRNN)

Spread values are; 10^{-7}, 10^{-8}, 10^{-9}, 10^{-10} for the training of $V_1, t_{appt1}, V_2, t_{appt2}$ and Nrs are 528 pieces (Number of input data) at the hidden layer. There is no performance difference between *spread* values.

Table 5
RBFN training data and results.

For the V_1 value,
- eg = 1.10^{-7}, sc = 2.10^{-7}, Nrs = 500, MSE = 1.01262e^{-05}
- eg = 1.10^{-8}, sc = 2.10^{-8}, Nrs = 500, MSE = 1.67582e^{-05}
- eg = 1.10^{-9}, sc = 2.10^{-9}, Nrs = 500, MSE = 1.94467e^{-05}
- eg = 1.10^{-10}, sc = 2.10^{-10}, Nrs = 500, MSE = 1.94467e^{-05}

For the t_{appt1} value,
- eg = 1.10^{-7}, sc = 2.10^{-7}, Nrs = 300, MSE = 2.44407e^{-07}
- eg = 1.10^{-8}, sc = 2.10^{-8}, Nrs = 500, MSE = 1.54078e^{-08}
- eg = 1.10^{-9}, sc = 2.10^{-9}, Nrs = 500, MSE = 1.25132e^{-07}
- eg = 1.10^{-10}, sc = 2.10^{-10}, Nrs = 500, MSE = 4.46526e^{-08}

For the V_2 value,
- eg = 1.10^{-7}, sc = 2.10^{-7}, Nrs = 350, MSE = 1.59203e^{-04}
- eg = 1.10^{-8}, sc = 2.10^{-8}, Nrs = 350, MSE = 1.59203e^{-04}
- eg = 1.10^{-9}, sc = 2.10^{-9}, Nrs = 350, MSE = 1.59203e^{-04}
- eg = 1.10^{-10}, sc = 2.10^{-10}, Nrs = 350, MSE = 1.59203e^{-04}

For the t_{appt2} value,
- eg = 1.10^{-7}, sc = 2.10^{-7}, Nrs = 50, MSE = 1.53781e^{-06}
- eg = 1.10^{-8}, sc = 2.10^{-8}, Nrs = 250, MSE = 2.40504e^{-07}
- eg = 1.10^{-9}, sc = 2.10^{-9}, Nrs = 450, MSE = 7.65449e^{-09}
- eg = 1.10^{-10}, sc = 2.10^{-10}, Nrs = 450, MSE = 1.76945e^{-07}

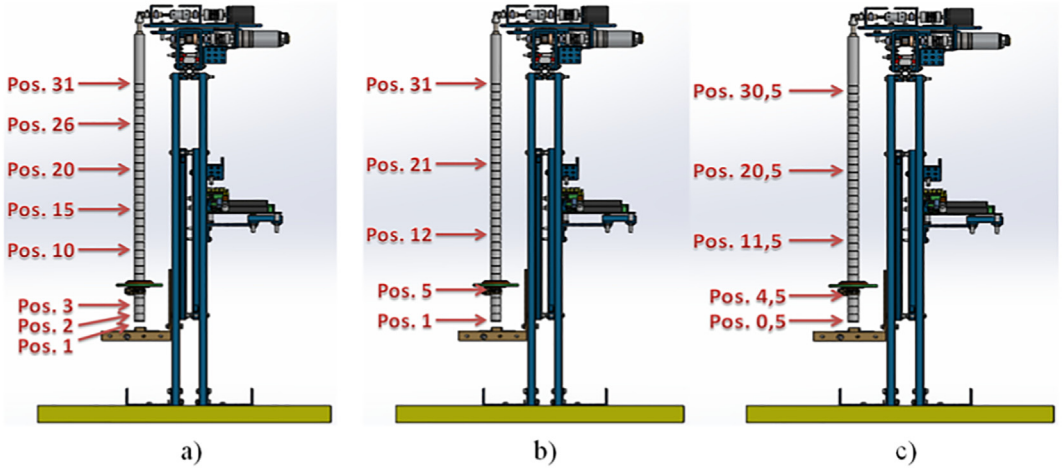


Fig. 10. Simple pendulum: a) Measuring points, b) Training points, c) Testing points.

4.2.3. Radial basis function network (RBFN)

Although they have dissimilar software lines, the training performance results of Underlapping Nrs (RBUN), Overlapping Nrs (RBON) and Approximation Nrs (RBAN) were the same. The Nrs number in the hidden layer is listed below. There are performance differences (MSE) between different sum-squared error goal values and *spread* values. Also, eg (Sum-squared error goal) and sc (*Spread* constant) are the main parameters as in (Table 5).

4.3. Experiment

As seen in Fig. 10(b) and Fig. 10(c), there are five critical points identified for experimental studies. The points in Fig. 10(b) are the places that we used before during the training and the points in Fig. 10(c) are the test points that have never been used before. Heights used in Fig. 10(b) are; 0, 1, 46.66, 128.33, 233.33, 350 mm and training weights are; 0, 8,16, 21, 29, 37, 42, 50, 58, 63, 71, 79, 84, 92, 100, 105, 113, 121 g. Heights used in Fig. 10(c) are; 0.5, 40.83, 122.49, 227.49, 344.16 mm and testing weights are; 14, 18,25, 34, 40, 46, 54, 61, 68, 74, 83, 88, 96, 103, 109, 117, 123 g. Total data for the training are 86 lines (17x5 = 85 + 1(Loadless) = 86) and total data for the testing are 85 lines (17x5 = 85). All tests are shown in Fig. 11 and Fig. 14.

4.3.1. Training

As seen in Fig. 11, all experiment graphics are the same but training rates are 85%, 99%, 100% and 100%. Apparently, the second stage of artificial intelligence applications has increased the level of training considerably. As seen in Fig. 12, the variable eg (Sum-Squared Error Goal for GRNN and RBFN) and sc (*Spread* Constant for only RBFN) values percentages of training are the same. These success rates were determined according to the graph results shown in Fig. 13. At the end of the sixth second, the amount of oscillation in Fig. 13(a) is extremely low. Showing the same amount of release was considered successful. At a distance of 200 mm, the pendulum's swing angle ranges from +7.2^0 degree to -7.2^0 degree and residual oscillation ranges from 0^0 degree to +1.8^0 degree now. Oscillation angle values other than these residual oscillation angle values considered unsuccessful. Training success rates of the NN, NN + NN, NN + GRNN(10^{-7}), NN + GRNN(10^{-8}), NN + GRNN(10^{-9}), NN + GRNN(10^{-10}), NN + RBUN, RBON, RBAN (10^{-7}), NN + RBUN, RBON, RBAN(10^{-8}), NN + RBUN, RBON, RBAN(10^{-9}), NN + RBUN, RBON, RBAN(10^{-10}) are 73/86, 85/86, 86/86, 86/86, 86/86, 86/86, 85/86, 86/86, 86/86, 86/86, respectively. Also, first stage NN training graphics results and second stage NN, GRNN, RBUN, RBON, RBAN training, and testing graphics results

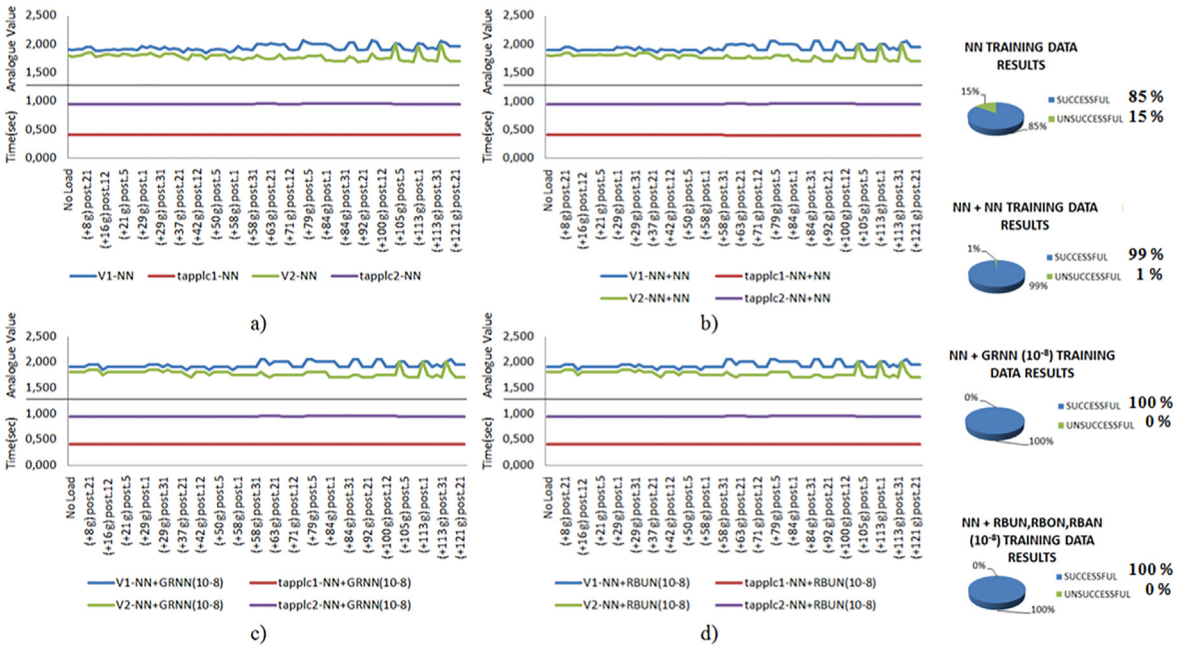


Fig. 11. Graphical results of training experiment.

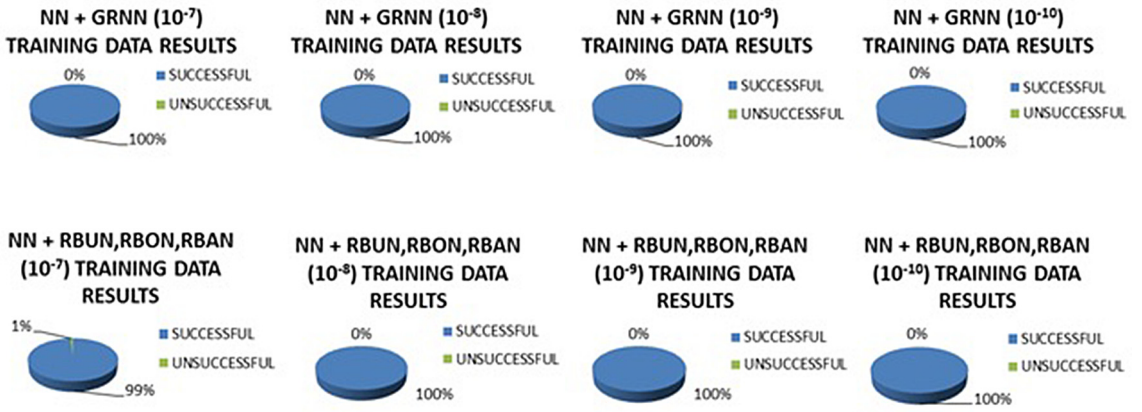


Fig. 12. Other training experiment results.

can be seen from the link below; https://drive.google.com/drive/folders/1QyX-PuDW2FG1rZ5zKQ5xjSCNW6Sv8Vya?usp=sharing.

4.3.2. Testing

As seen in Fig. 14, all experiment graphics are the different in overall outlook. Testing rates are 53%, 78%, 96% and 46%. Apparently, only one artificial intelligence application has maintained the level of testing considerably. As seen in Fig. 15, with variable eg (Sum-Squared Error Goal for GRNN and RBFN) and sc (*Spread* Constant for only RBFN) values, percentages of testing are different. These percentages were determined according to the graph results shown in Fig. 16. At the end of the 7th second, the amount of oscillation in Fig. 16(a) is extremely low. Tests showing the same amount of release were considered successful. At a distance of 200 mm, the pendulum's swing angle ranges from $+7.2^0$ degree to -7.2^0 degree. Residual oscillation ranges from 0^0 degree to $+1.8^0$ degree. Oscillation angle values other than these residual oscillation angle values considered unsuccessful. Testing success rates of the NN, NN + NN, NN + GRNN(10^{-7}), NN + GRNN(10^{-8}), NN + GRNN(10^{-9}), NN + GRNN(10^{-10}), NN + RBUN, RBON, RBAN (10^{-7}), NN + RBUN, RBON, RBAN(10^{-8}), NN + RBUN, RBON, RBAN(10^{-9}), NN + RBUN, RBON, RBAN(10^{-10}) are 45/85, 66/85, 82/85, 82/85, 82/85, 82/85, 45/85, 39/85, 37/85, 38/85, respectively. Also,

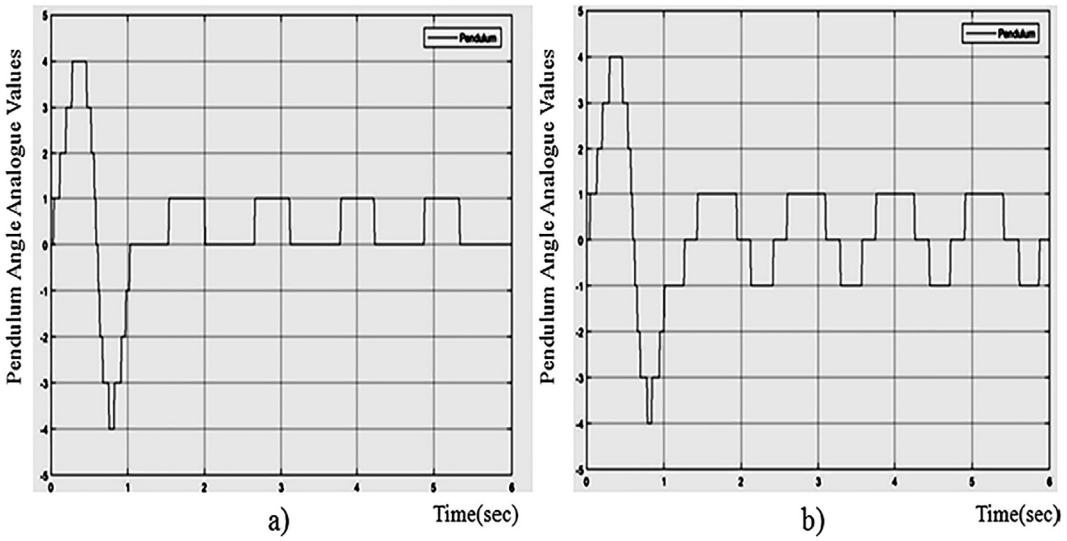


Fig. 13. Pendulum oscillation training graphics: a) Successful, b) Unsuccessful (Sample time = 0.01 sec.).

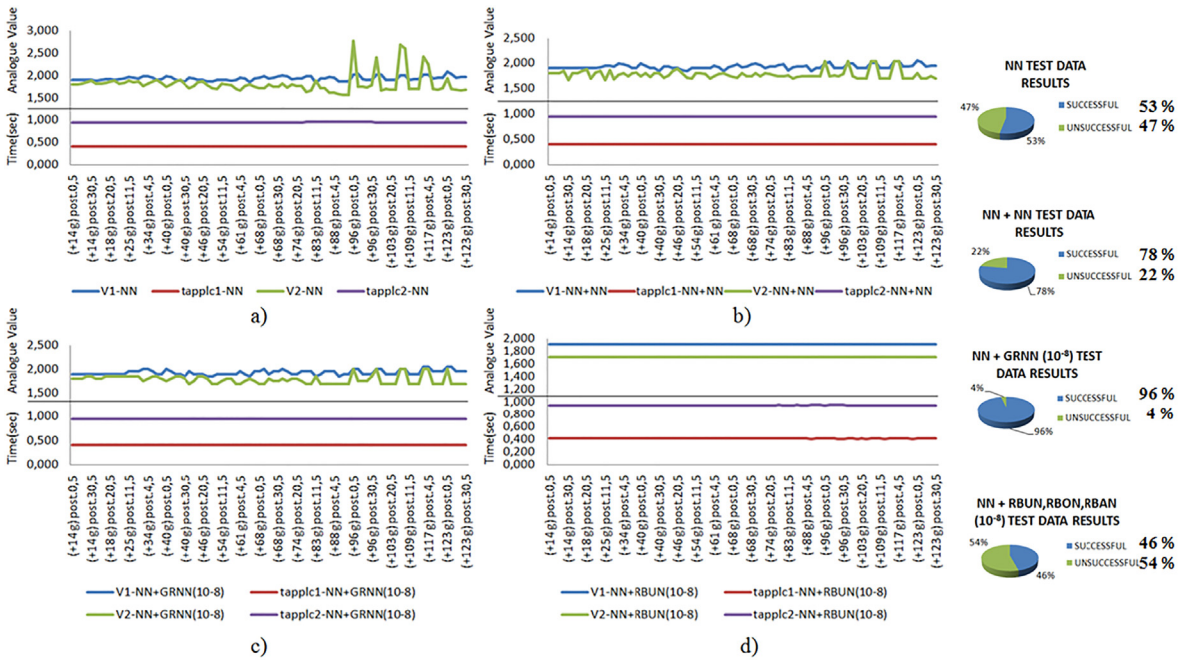


Fig. 14. Graphical results of testing experiment.

first stage NN training graphics results and second stage NN, GRNN, RBUN, RBON, RBAN training, and testing graphics results can be seen from the link below;

https://drive.google.com/drive/folders/1QyX-PuDW2FG1rZ5zKQ5xjSCNW6Sv8Vya?usp=sharing.

5. Results and discussions

Single-layer NN training with 528 lines of data has achieved with success rates ranging from 94% to 100%. These values were not enough to find the application time periods exactly. Due to the low amount of data, adding additional hidden layers to the NNs or rising the number of Nrs at the hidden layers did not change the results. At this point, hybrid methods were mandatory. As mentioned in Section 2, the success rates of Probabilistic Neural Networks (PNNs) that is GRNNs and RBFNs

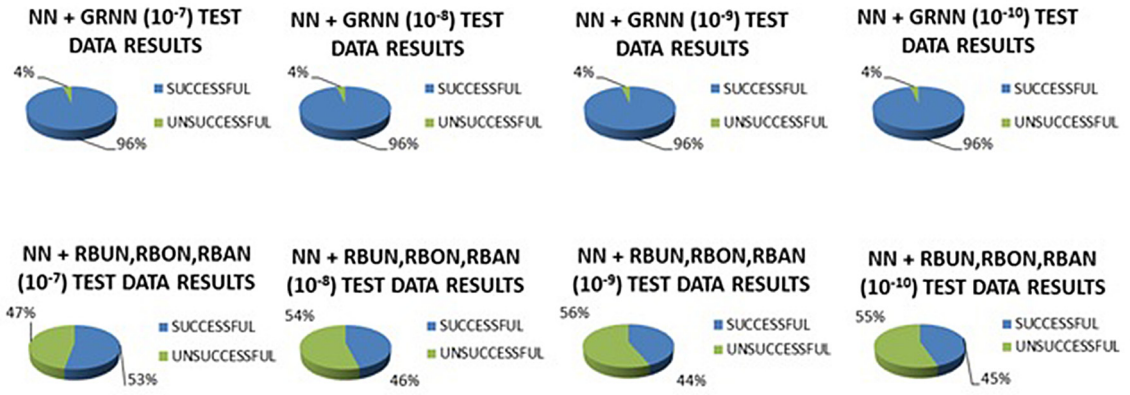


Fig. 15. Other testing experiment results.

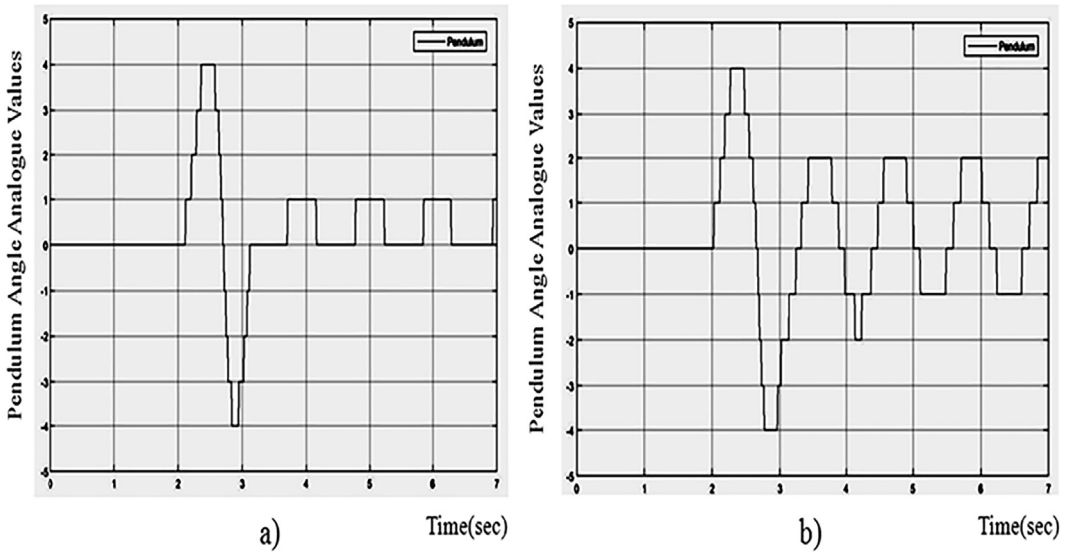


Fig. 16. Pendulum oscillation testing graphics: a) Successful, b) Unsuccessful (Sample time = 0.01sec.).

are very high. Also, they have proven themselves in studies on the inverted pendulum. Therefore, they were inevitable to be successful in IS applications. The combination of these networks with other NNs increased in importance. As a result, residual oscillations at the pendulum's endpoint could be minimized by the pulses at the right time and at the right speed with these combinations successfully.

According to the experimental results, it was seen that the training results and testing results were quite different from each other. The most successful work in the series was realized in cooperation with NN + GRNN. Also, the average distances taken during the testing are shown in Fig. 17. NN + GRNN cooperated again had the same success about the closest distance to 200 mm ideal working distance with an average 0.203 m. Great training performance of RBFN was not achieved at the testing data performances. While *spread* constant value was increasing especially at the training experiments we saw that the results were more successful. But the same success was not seen at the testing performances. The same failure was seen at the average movement distances too. In the second stage, the use of the second single-layer NN was able to increase the success rate only to a certain point and its average movement distance was below the desired level.

It took an average of 0.66 h to find the best impulse and application times for a weight added to the pendulum during the studies. The total time spent on training data is 0.66x528 = 348.48 h. These times can be reduced a sensible levels by practical applications and in more sensitive experimental sets. The other shortcoming of the current study is that it does not provide robustness against external forces. For this, apart from some of the hybrid methods mentioned in section 2 [16,25], many studies based on SMC similar drawbacks [19,24,67,68]. Adaptive control methods have also been developed, which can meet parameter uncertainties, external disturbances and even one-way restrictions [69,70]. They can even have a continuous expression that is smoother than traditional SMC [70]. Ultimately, in all methods, an additional oscillation angle

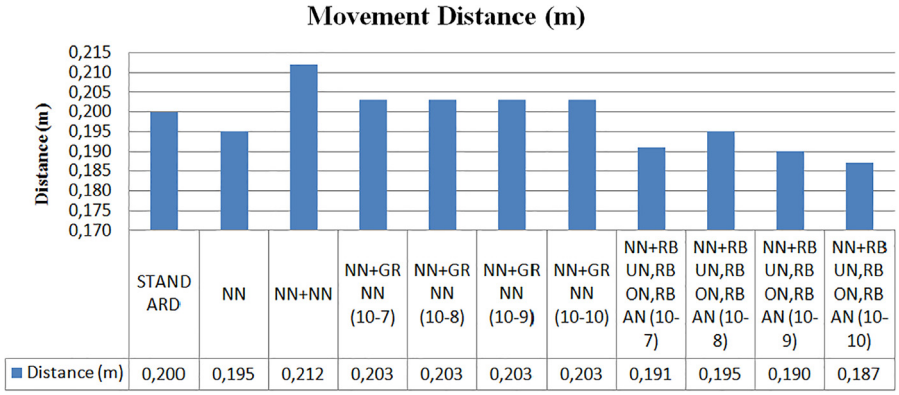


Fig. 17. Average movement distance (m).

caused by external disturbances can be observed, albeit for a certain period of time. In future studies, a more effective damping method will be studied against these external forces.

6. Conclusion

The most effective load-bearing method in cranes is defined to minimize load oscillations [45]. The movement of a crane is prone to overload release due to its structure. This situation naturally affects position accuracy, effectiveness and safety of the operations. If the oscillation angles cannot be controlled, there may be difficulties in automation by the worker, damage to the transported load and even the toppling of the crane is possible. In addition, the work takes a lot of time to complete and effective working speed is reduced. According to statistics, conventional placement equipment wastes more than 30% of its operational times for fixing the payload per the loading time [71]. Therefore, it is necessary to use intelligent control methods in the most efficient way in order to avoid loss of time while carrying the load. As a result, in spite of the small amount of training data, pendulum positioning has been performed successfully thanks to cooperation with NN + GRNN. The same success was observed in average movement distances. The experimental results indicate that the proposed approach achieves the aimed objective very well.

Information

The work belongs to the doctoral graduation project. No financial support was received from any organization.

Declaration of Competing Interest

The authors declare that they have no known competing financial interests or personal relationships that could have appeared to influence the work reported in this paper.

References

[1] Crane Konecranes control systems. <https://www.konecranes.com.tr/> (accessed 2018 03.11.18)
[2] J. Vaughan, A. Karajgikar, W. Singhose, A Study of Crane Operator Performance Comparing PD-Control and Input Shaping, in: 2011 Am. Control Conf., San Francisco, USA, 2011: pp. 545–550.
[3] A. Takemoto, K. Yano, T. Miyoshi, K. Terashima, Operation Assist Control System of Rotary Crane Using Proposed Haptic Joystick as a Man-Machine Interface, in: 13th IEEE Int. Work. Robot Hum. Interact. Commun., Okayama, Japan, 2004: pp. 533–538.
[4] A. Khalid, J. Huey, W. Singhose, J. Lawrence, D. Frakes, Human Operator Performance Testing Using an Input-Shaped Bridge Crane, J. Dyn. Syst. Meas. Control-Trans., ASME. 128 (2006) 835–841.
[5] İ. Yüksel, Otomatik Kontrol Sistem Dinamiği ve Denetim Sistemleri, Nobel Akademik Yayıncılık (2011).
[6] H. Saeidi, M. Naraghi, A.A. Raie, A neural network self tuner based on input shapers behavior for anti sway system of gantry cranes, J. Vib. Control 19 (2013) 1936–1949.
[7] J. Stergiopoulos, A. Tzes, An Adaptive Input Shaping Technique for the Suppression of Payload Swing in Three-Dimensional Overhead Cranes with Hoisting Mechanism, IEEE. (2007), 1-4244-0826-1/07/$20.00.
[8] D. Fujioka, W. Singhose, Performance comparison of input-shaped model reference control on an uncertain flexible system, Res. Gate. (2015), https://doi.org/10.1016/j.ifacol.2015.09.365.
[9] D. Fujioka, M. Shah, W. Singhose, Robustness Analysis of Input-Shaped Model Reference Control on a Double-Pendulum Crane, AACC. (2015), 978-1-4799-8684-2/$31.00.
[10] D. Qıan, S. Tong, B. Yang, S. Lee, Design of Simultaneous Input-Shaping-Based Sırms Fuzzy Control for Double Pendulum-Type Overhead Cranes, Bull. Pol. Ac. (2015) Tech. 63 (4).
[11] K. Sorensen, H. Fisch, S. Dickerson, W. Singhose, U. Glauser, A Multi Operational-Mode Anti-Sway and Positioning Control for an Industrial Bridge Crane, IFAC. (2008), 978-1-1234-7890-2/08/$20.00.

[12] M. Kenison, W. Singhose, Concurrent design of input shaping and proportional plus derivative feedback control, J. Dyn. Syst. Meas. Contr. 124 (2002) 398–405.
[13] M.J. Maghsoudi, L. Ramli, S. Sudin, Z. Mohamed, A.R. Husain, H. Wahid, Improved Unity Magnitude Input Shaping Scheme for Sway Control of an Underactuated 3D Overhead Crane with Hoisting, Mech. Syst. Sig. Process. 123 (2019) 466–482.
[14] L. Ramli, Z. Mohamed, H.I. Jaafar, A neural network-based input shaping for swing suppression of an overhead crane under payload hoisting and mass variations, Mech. Syst. Sig. Process. 107 (2018) 484–501.
[15] M.J. Maghsoudi, Z. Mohamed, S. Sudin, S. Buyamin, H.I. Jaafar, S.M. Ahmad, An Improved Input Shaping Design for an Efficient Sway Control of a Nonlinear 3D Overhead Crane with Friction, Mech. Syst. Sig. Process. 92 (2017) 364–378.
[16] L. Ramli, Z. Mohamed, M.Ö. Efe, I.M. Lazim, H.I. Jaafar, Efficient swing control of an overhead crane with simultaneous payload hoisting and external disturbances, Mech. Syst. Sig. Process. 135 (2020) 106326.
[17] H.I. Jaafar, Z. Mohamed, M.A. Shamsudin, N.A.M. Subha, L. Ramli, A.M. Abdullahi, Model reference command shaping for vibration control of multimode flexible systems with application to a double-pendulum overhead crane, Mech. Syst. Sig. Process. 115 (2019) 677–695.
[18] M.J. Maghsoudi, Z. Mohamed, A.R. Husain, M.O. Tokhi, An optimal performance control scheme for a 3D crane, Mech. Syst. Sig. Process. 66–67 (2016) 756–768.
[19] M.-C. Pai, Robust input shaping control for multi-mode flexible structures, Int. J. Control Autom. Syst. 9 (1) (2011) 23–31.
[20] S. Arabasi, Z. Masoud, Simultaneous travel and hoist maneuver input shaping control using frequency modulation, Shock Vib. 2017 (2017) 1–12, https://doi.org/10.1155/2017/5703820.
[21] R. Mar, A. Goyal, V. Nguyen, T. Yang, W. Singhose, Combined input shaping and feedback control for double-pendulum systems, Mech. Syst. Sig. Process. 85 (2017) 267–277.
[22] M. Z. M. Tumari, L. Shabudin, M. A. Zawawi, L. H. A. Shah, Active Sway Control of a Gantry Crane Using Hybrid Input Shaping and PID Control Schemes, 2nd International Conference on Mechanical Engineering Research (ICMER 2013), IOP Conf. Series: Materials Science and Engineering. 50 (2013) 012029.
[23] M. A. Ahmad, A. N. K. Nasir, N. Hambali, H. Ishak, Hybrid Input Shaping and PD-Type Fuzzy Logic Control Scheme of a Gantry Crane System, 18th IEEE International Conference on Control Applications Part of 2009, IEEE Multi-Conference on Systems and Control, Saint Petersburg, Russia, 2009.
[24] M.-C. Pai, Closed-Loop Input Shaping Control of Vibration in Flexible Structures Via Adaptive Sliding Mode Control, ISSN 1070–9622/12, Shock Vib. 19 (2012) 221–233.
[25] W. Chatlatanagulchai, Model Reference Input Shaping Using Quantitative Feedforward-Feedback Controller, ISSN 0125-8281, Engineering Journal. (2017), V. 21 Is. 1.
[26] R. Ghorbani, Q. Wu, G.G. Wang, Nearly optimal neural network stabilization of bipedal standing using genetic algorithm, Eng. Appl. Artif. Intell. 20 (2007) 473–480.
[27] M. Stogiannos, A. Alexandridis, H. Sarimveis, Model predictive control for systems with fast dynamics using inverse neural models, ISA Trans. 72 (2018) 161–177.
[28] X.-S. Wang, Y.-H. Cheng, J.-Q. Yi, A Fuzzy actor-critic reinforcement learning network, Inf. Sci. 177 (2007) 3764–3781.
[29] H.-M. Feng, Self-Generation RBFNs Using Evolutional PSO Learning, Neurocomputing. 70 (2006) 241–251.
[30] Pololu, Brushed DC motor with encoder. <https://www.pololu.com/product/3213>, 2018 (accessed 22.12.18).
[31] Pololu, Motor controller card. <https://www.pololu.com/product/1383>, 2018 (accessed 22.12.18).
[32] Sparkfun, Rotary encoder. <https://static.sparkfun.com/datasheets/Robotics/E6A2%20 encoder.pdf>, 2019 (accessed 07.01.19).
[33] Humusoft, Data acquisition card. <https://www.humusoft.cz/datacq/mf634/>, 2018 (accessed 11.06.18).
[34] L. Ramli, Z. Mohamed, A.M. Abdullahi, H.I. Jaafar, I.M. Lazim, Control Strategies for Crane Systems: A Comprehensive Review, Mech. Syst. Sig. Process. 95 (2017) 1–23.
[35] Probabilistic Wisconsin neural networks. <https://minds.wisconsin.edu/bitstream/ (accessed handle/1793/7779/ch2.pdf?sequence=14>, 2019 15.04.19)
[36] J. Vaughan, W. Singhose, Input Shapers for Reducing Overshoot in Human-Operated Flexible Systems, in: 2009 Am. Control Conf., IEEE, New York, USA, 2009: pp. 178–183.
[37] D. Kim, W. Singhose, Performance studies of human operators driving double-pendulum bridge cranes, Control Eng. Pract. 18 (2010) 567–576.
[38] D. Kim, W. Singhose, Studies of Human Operators Manipulating Double-Pendulum Bridge Cranes, in: Eur. Control Conf., Greece, ECC 2007: pp. 3471–3478.
[39] D. Kim, W. Singhose, Human Operator Learning on Double-Pendulum Bridge Cranes, in: ASME Int. Mech. Eng. Congr. Expo. Proc., Washington, USA, 2008: pp. 1959–1965.
[40] A. Karajgikar J. Vaughan W. Singhose . Shaping, in: ECCOMAS Themat. Conf., Double Pendulum Crane Operator Performance Comparing PD-Feedback Control and Input 2011 Brussels, Belgium 1 14
[41] Ç. Conker H. Yavuz S. Kapucu M.K. Baltacıoğlu H.T. Arat A. Burgaç Comparison of Robust Input Shapers for Elimination of Residual Vibrations Applied Mechanics and Materials. 2014 490–491.997
[42] Ç. Conker, H. Yavuz, H. H. Bilgiç, A Review of Command Shaping Techniques for Elimination of Residual Vibrations in Flexible-Joint Manipulators, JVE International Ltd. Journal of Vibroengineering. (2016) V. 18, I. 5. ISSN 1392-8716.
[43] Prof. Dr. E. Öztemel, Yapay Sinir Ağları, Papatya Yayıncılık, İstanbul, 2012.
[44] E. Al-Daoud, A comparison between three neural network models for classification problems, J. Artif. Intell. 2 (2009) 56–64.
[45] D.F. Specht, A general regression neural network, IEEE Trans. Neural Networks 2 (6) (1991) 568–576.
[46] T. Kiyan, T. Yildirim, Breast cancer diagnosis using statistical neural networks, J. Electr. Electronics Eng. 4 (2) (2004) 1149–1153.
[47] N. Currit, Inductive Regression: Overcoming OLS Limitations with the General Regression Neural Network, Comput. Environ. Urban Syst. 26 (2002) 335–353.
[48] V.K. Alilou, F. Yaghmaee, Application of GRNN Neural Network in Non-Texture Image Inpainting and Restoration, Pattern Recogn. Lett. 62 (2015) 24–31.
[49] Z. Xiao-hong, W. Qi-jie, Z. Jian-jun, Z. Hao, Application of General Regression Neural Network to the Prediction of LOD Change, Chin. Astron. Astrophy 36 (2012) 86–96.
[50] M. Firat, M. Gungor, Generalized regression neural networks and feed forward neural networks for prediction of scour depth around bridge piers, Adv. Eng. Softw. 40 (2009) 731–737.
[51] M.M. Islam, G. Lee, S.N. Hettiwatte, Application of a general regression neural network for health index calculation of power transformers, Electr. Power Energy Syst. 93 (2017) 308–315.
[52] H. Bendu, B.B.V.L. Deepak, S. Murugan, Application of GRNN for the Prediction of Performance and Exhaust Emissions in HCCI Engine Using Ethanol, Energy Convers. Manage. 122 (2016) 165–173.
[53] L. Y. Fannas, A. Y. B. Sasi, Off-Line Signature Recognition Based on Angle Features and GRNN Neural Networks, World Academy of Science, Engineering and Technology International Journal of Computer and Information Engineering. (2013), V. 7, N. 10.
[54] M.R. Obeıdavı, A. Rafıee, O. Mahdıyar, Diagnosing Thyroid Disease by Neural Networks, Biomedical & Pharmacology Journal. 10 (2) (2017) 509–524.
[55] Ş. Sağıroğlu, E. Beşdok, M. Erler, Mühendislikte Yapay Zeka Uygulamaları I, Yapay Sinir Ağları, UFUK Yayıncılık, 2003.
[56] Kipdf, Structure of GRNN. <https://kipdf.com/queue/radial-basis-networks_5ab1037e1 723dd339c806842.html>, 2019 (accessed 19.07.19).
[57] D. Tomandl, A. Schober, A Modified General Regression Neural Network with New Efficient Training Algorithms as a Robust 'Black Box'-Tool for Data Analysis, Neural Networks. 14 (2001) 1023–1034.
[58] Structure Edoras of RBF. <https://edoras.sdsu.edu/doc/matlab/toolbox/nnet/radial78.html> (accessed 2019 23.07.19)

[59] D.F. Specht, Probabilistic Neural Networks, Neural Networks. 3 (1) (1990) 109–118.
[60] A. J. Al-Mahasneh, S. G. Anavatti, M. A. Garratt, Review of Applications of Generalized Regression Neural Networks in Identification and Control of Dynamic Systems. arXiv:1805.11236v1 [cs.NE] 2018.
[61] A. Sahroni, Design of Intelligent Control System Based on General Regression Neural Network Algorithm, GSTF Journal on Computing (JoC). (2013), V. 2, N. 4.
[62] J. Moody, C. J. Darken, Fast Learning in Networks of Locally-Tuned Processing Units, Neural Computation. V. (1) 1989: pp. 281-294.
[63] M.J.D. Powell, Restart Procedures for The Conjugate Gradient Method, Math. Program. 12 (1977:) 241–254.
[64] D.S. Broomhead, D. Lowe, Multivariable Functional Interpolation and Adaptive Networks, Complex Systems. 2 (1988:) 321–355.
[65] X. Zhu, N. Wang, Cuckoo Search Algorithm with Membrane Communication Mechanism for Modeling Overhead Crane Systems Using RBF Neural Networks, Appl. Soft Comput. 56 (2017) 458–471.
[66] Researchgate, Structure of RBFN. <https://www.researchgate.net/publication/303826547_Artificial_Neural_Networks_Part_7Radial_Basis_Function_Networks_RBFNs>, 2019 (accessed 13.10.19).
[67] L.A. Tuan Q. Ha P.V. Trieu Observer-Based Nonlinear Robust Control of Floating Container Cranes Subject to Output Hysteresis Journal of Dynamic Systems, Measurement, and Control. V 2019 141/111002-1
[68] L.A. Tuan, Fractional-Order Fast Terminal Back-Stepping Sliding Mode Control of Crawler Cranes, Mech. Mach. Theory 137 (2019) 297–314.
[69] T. Yang, N. Sun, H. Chen, Y. Fang, Neural Network-Based Adaptive Antiswing Control of an Underactuated Ship-Mounted Crane with Roll Motions and Input, Dead Zones, IEEE Transactions on Neural Networks and Learning Systems. (2019) 2162–2237.
[70] Ning Sun Dingkun Liang Yiming Wu Yiheng Chen Yanding Qin Yongchun Fang Adaptive Control for Pneumatic Artificial Muscle Systems With Parametric Uncertainties and Unidirectional Input Constraints IEEE Trans. Ind. Inf. 16 2 2020 969 979 10.1109/TII.9424 10.1109/TII.2019.2923715 https://ieeexplore.ieee.org/xpl/RecentIssue.jsp?punumber=9424 https://ieeexplore.ieee.org/document/8740896/
[71] C. Liu, H. Zhao, Y. Cui, Research on Application of Fuzzy Adaptive PID Controller in Bridge Crane Control System, in: 2011 Int. Conf. Control. Autom. Syst. Eng., IEEE, Beijing, China, 2011: pp. 1–4.